© 2004 by the American College of Cardiology Foundation
Published by Elsevier Inc.

ISSN 0735-1097/04/$30.00
doi:10.1016/j.jacc.2004.01.048

Characteristics of Virtual Unipolar Electrograms for Detecting Isthmus Block During Radiofrequency Ablation of Typical Atrial Flutter

Yenn-Jiang Lin, MD,* Ching-Tai Tai, MD,* Jin-Long Huang, MD,† Tu-Ying Liu, MD,* Pi-Chang Lee, MD,* Chih-Tai Ting, MD, PHD,† Shih-Ann Chen, MD*

Taipei and Taichung, Taiwan

OBJECTIVES The purpose of this study was to investigate the characteristics of the second component of local virtual unipolar electrograms recorded at the ablation line during coronary sinus (CS) pacing after radiofrequency ablation (RFA) of the cavotricuspid isthmus (CTI) for typical atrial flutter (AFL).

BACKGROUND Radiofrequency ablation of the CTI can produce local double potentials at the ablation line. The second component of unipolar electrograms represents the approaching wavefront in the right atrium opposite the pacing site. We hypothesized that the morphologic characteristics of the second component of double potentials would be useful in detecting complete CTI block.

METHODS Radiofrequency ablation of the CTI was performed in 52 patients (males = 37, females = 15, 62 ± 12 years) with typical AFL. The noncontact mapping system (Ensite 3000, Endocardial Solutions, St. Paul, Minnesota) was used to guide RFA. Virtual unipolar electrograms along the ablation line during CS pacing after RFA were analyzed. Complete or incomplete CTI block was confirmed by the activation sequence on the halo catheter and noncontact mapping.

RESULTS Three groups were classified after ablation. Group I (n = 37) had complete bidirectional CTI block. During CS pacing, the second component of unipolar electrograms showed an R or Rs pattern. Group II (n = 12) had incomplete CTI block. The second component of unipolar electrograms showed an rS pattern. Group III (n = 3) had complete CTI block with transcristal conduction. The second component of unipolar electrograms showed an rSR pattern.

CONCLUSIONS A predominant R-wave pattern in the second component of unipolar double potentials at the ablation line indicates complete CTI block, even in the presence of transcristal conduction. (J Am Coll Cardiol 2004;43:2300–4) © 2004 by the American College of Cardiology Foundation

Previous studies have demonstrated that typical atrial flutter (AFL) is due to a cavotricuspid isthmus (CTI)-dependent reentry circuit in the right atrium (RA), and creation of complete CTI conduction block can prevent recurrence of AFL (1–8). Although activation mapping using the halo catheter may be the gold standard for detecting complete CTI block, transverse conduction across the crista terminalis (CT) will affect the activation sequence around the tricuspid annulus mimicking incomplete CTI block (9,10). On the other hand, local wide double potentials were considered as criteria for diagnosis of complete CTI block (11). However, ambiguous electrograms cannot exclude the possibility of very slow conduction (10). Moreover, change of contact unipolar electrograms in the RA opposite the pacing site seems to be useful for detecting complete CTI block after radiofrequency ablation (RFA) of the CTI (12).

The noncontact mapping system has been demonstrated to facilitate RFA of typical AFL because it shows simultaneous three-dimensional activation in the whole RA (13,14). Furthermore, this system also can show local virtual unipolar electrograms along the ablation line. Because the second component of local double potentials after RFA of the CTI represents the approaching wavefront in the RA opposite the pacing site, we hypothesized that the morphologic characteristics of the second component electrograms would be useful for detecting complete CTI block. Therefore, the purpose of this study was to investigate the characteristics of the second component of local double potentials recorded at the ablation line after RFA of the CTI in patients with typical AFL using the noncontact mapping system.

From the *Division of Cardiology, Department of Medicine, National Yang-Ming University School of Medicine, Taipei Veterans General Hospital, Taipei, Taiwan; and †Taichung Veterans General Hospital, Taichung, Taiwan. Supported, in part, by grants from National Science Council (NSC 90-2314-B-010-023, 90-2314-B-075-044, 90-2315-B-010-004) and Taichung Veterans General Hospital (TCVGH-913101B, 923103B), Taiwan, R.O.C.

Manuscript received December 15, 2003; revised manuscript received January 19, 2004, accepted January 31, 2004.

METHODS

Patient characteristics. The study population consisted of 52 patients (mean age, 62 ± 12 years; males = 37, females = 15) with clinically documented AFL referred for RFA. Eleven patients had structural heart disease, including six with hypertension, two with ischemic heart disease, two with valvular heart diseases, and one with congenital heart disease.

Catheter position and electrophysiologic study. Informed, written consent was obtained from all patients. As described previously, all antiarrhythmic drugs were discontinued for at least five half-lives before the study (8,15). In all patients, a 7F, 20-pole, deflectable halo catheter with 10-mm paired

Abbreviations and Acronyms

AFL = atrial flutter
CS = coronary sinus
CT = crista terminalis
CTI = cavotricuspid isthmus
IVC = inferior vena cava
MEA = multielectrode array
RA = right atrium
RFA = radiofrequency ablation

spacing (Cordis-Webster Inc., Baldwin Park, California) was positioned around the tricuspid annulus to record the RA activation at the lateral wall and the low RA isthmus simultaneously. A 7F, deflectable decapolar catheter with 2-mm interelectrode distance and 5-mm space between each electrode pair was inserted into the coronary sinus (CS) via the internal jugular vein. A 9F sheath was introduced to place the noncontact mapping electrode array in the RA by the femoral vein approach. If spontaneous AFL was found at the onset of study, multicatheter mapping and noncontact mapping were performed simultaneously to investigate the re-entry circuit. If sinus rhythm was present at baseline, atrial pacing from the CS and low RA was performed to induce AFL.

Noncontact mapping system. The noncontact mapping system (Ensite 3000, Endocardial Solutions, St. Paul, Minnesota) has been described in detail previously (15). In brief, the system consists of a noncontact catheter (9F) with a multielectrode array (MEA) surrounding a 7.5-ml balloon mounted at the distal end. Raw data detected by the MEA is transferred to a silicon graphics workstation via a digitalized amplifier system. Before the MEA catheter was deployed, patients were given 3,000 U of heparin, with subsequent boluses to maintain activated clotting time between 250 and 300 s. The MEA catheter was deployed over a 0.032-inch guidewire, which had been advanced to the superior vena cava. The system locates any catheter in relation to the MEA using an impedance-based "locator signal," that serves two purposes. First, it is used to construct a three-dimensional computer model of the virtual endocardium providing a geometry matrix for the inverse solution. To achieve this, geometric points are sampled at the beginning of the study during sinus rhythm or AFL. Second, the locator signal is also used to display and track the position of the catheter on the virtual endocardium and allows the marking of the catheter on the virtual endocardium and allows the marking of anatomic locations identified using fluoroscopy and electrogram characteristics.

Using mathematical techniques to process these potentials, the system is able to reconstruct more than 3,000 unipolar electrograms simultaneously and superimpose them onto the virtual endocardium, producing isopotential maps with a color range representing voltage amplitude. Reconstructed unipolar electrograms can also be judiciously selected from sites on the virtual endocardium and displayed individually.

RFA and follow-up. Radiofrequency energy was delivered using a quadripolar 8-mm tip electrode ablation catheter with temperature control (7F, EP Technologies Inc., Mountain View, California) to achieve a tip-tissue interface temperature of 70°C during AFL or sinus rhythm. The preset duration of each radiofrequency pulse was 120 s for each pulse. Radiofrequency energy was applied during pull-back of the ablation catheter from the right ventricle toward the inferior vena cava (IVC) to create linear lesions. After successful ablation of AFL, the electrophysiologic study was repeated to ensure complete bidirectional isthmus block using both contact (halo catheter) and noncontact mapping.

The complete clockwise CTI block was confirmed by the observation of a purely descending wavefront at the lateral wall down to the CTI during pacing from proximal CS (7,8). An incomplete clockwise CTI block was defined when a descending wavefront at the lateral wall still allowed the lateral part of the isthmus to be activated from the proximal CS, resulting in displacement of collision at the lower part of lateral RA (7,8). Positional pacing and noncontact mapping were performed to confirm complete CTI block with transcristal conduction (10).

After discharge, each patient was regularly evaluated in the clinics with history and physical examination. If patients experienced symptoms suggestive of tachycardia, 24-h Holter monitoring or cardiac event recorder was performed to define the causes of clinical symptoms. If patients had recurrent typical AFL, RFA might be repeated.

Definitions of unipolar and bipolar electrograms. The following definitions of unipolar waveforms were used:

RS: one positive deflection followed by a negative deflection with an R/S ratio = 1.

rS: one small positive deflection followed by a large negative deflection with r/S <1.

Rs: one large positive deflection followed by a small negative deflection with R/s >1.

QS: only one large negative deflection.

R: only one large positive deflection.

rSR: one small positive deflection followed by a negative deflection and then positive deflection.

Statistical analysis. Quantitative values are expressed as mean ± SD. Statistical comparison of age and flutter cycle length between the three groups was performed with the Kruskal-Wallis one-way analysis of variance test. A value of $p < 0.05$ was considered to be statistically significant.

RESULTS

Electrophysiologic characteristics before RFA. There were 9 patients with spontaneous AFL and 43 patients with inducible AFL at baseline. The mean AFL cycle length was

235 ± 31 ms (range, 187 to 300 ms). Noncontact mapping and halo catheter mapping showed counterclockwise AFL in 39 patients and clockwise AFL in 13 patients. Atrial pacing terminated tachycardia in all nine patients with spontaneous AFL. During CS pacing, noncontact mapping showed that one wavefront traveled through the CTI and the other wavefront propagated upward in the septum and downward in the free wall. Both wavefronts collided in the anterolateral wall. The virtual unipolar electrograms in the CTI showed an RS (n = 9), rS (n = 41), or QS (n = 2) pattern.

Electrophysiologic characteristics after RFA. After a mean of 5 ± 3 radiofrequency pulses, 37 patients had complete bidirectional CTI block (group I), 12 patients had incomplete CTI block (group II), and 3 patients had complete bidirectional CTI block with transverse conduction in the CT mimicking CTI conduction (group III). There was no significant difference in age (p = 0.6) and AFL cycle length (p = 0.36) between the three groups.

GROUP I (N = 37). After RFA, double potentials were found at the ablation line with a mean interval of 103 ± 16 ms (range, 82 to 120 ms) during CS pacing. The second component of double potentials showed an R (n = 30) or Rs (n = 7) pattern. The mean R/s ratio was 4.7 ± 0.6 (range, 4.2 to 5.9). Noncontact mapping demonstrated that one wavefront blocked in the CTI and the other wavefront propagated upward in the septal wall, over the top of the CT and downward in the anterolateral wall (Fig. 1).

GROUP II (N = 12). After RFA, double potentials were also found at the ablation line with a mean interval of 43 ± 7 ms (range, 34 to 55 ms) during CS pacing. The second component of double potentials showed an rS pattern in all 12 patients. The mean r/S ratio was 0.4 ± 0.2 (range, 0.2 to 0.7). Noncontact mapping demonstrated that one wavefront traveled slowly through the CTI conduction gap and the other wavefront propagated upward in the septal wall and downward in the free wall. Both wavefronts collided in the low anterolateral wall (Fig. 2).

GROUP III (N = 3). After RFA, double potentials were found at the ablation line with a mean interval of 41 ± 10 ms (range, 29 to 52 ms) during CS pacing. The second component of double potentials showed an rSR pattern in all three patients. Noncontact mapping demonstrated that one wavefront blocked in the CTI, the other wavefront propagated through a conduction gap in the CT, and another wavefront went upward in the septal wall and downward in the free wall. These sequential approaching wavefronts produced an rSR pattern in the second component at ablation site in three patients (Fig. 3).

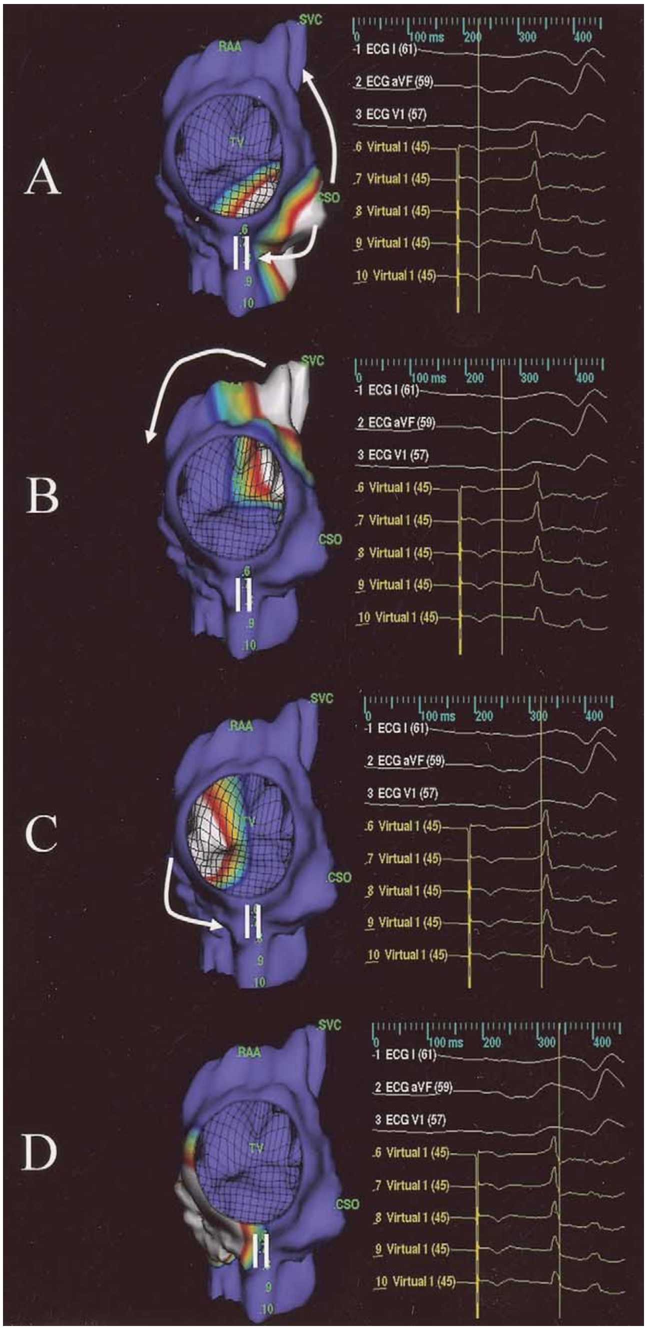

Figure 1. Complete cavotricuspid isthmus block during coronary sinus (CS) pacing after ablation. **(A)** After ablation, the activation wavefront originated in the CS ostium region blocked at the ablation line and propagated upward the septal wall. **(B)** The activation wavefront activated the roof and crossed the top of the crista terminalis. **(C)** The activation wavefront activated the high anterolateral wall and propagated downward. **(D)** The activation wavefront activated the low anterolateral wall and ended at the ablation line. The second component of virtual electrograms (virtual 6 to 10) at the ablation line showed an Rs pattern.

DISCUSSION

Major findings. This study demonstrated the usefulness of virtual unipolar electrograms (second component of double potentials) at the ablation line for detecting CTI block after RFA of typical AFL. During CS pacing, patients with complete CTI block had an R or Rs pattern. Patients with an incomplete CTI block had an rS pattern. Patients with a complete CTI block and transcristal conduction had an rSR pattern.

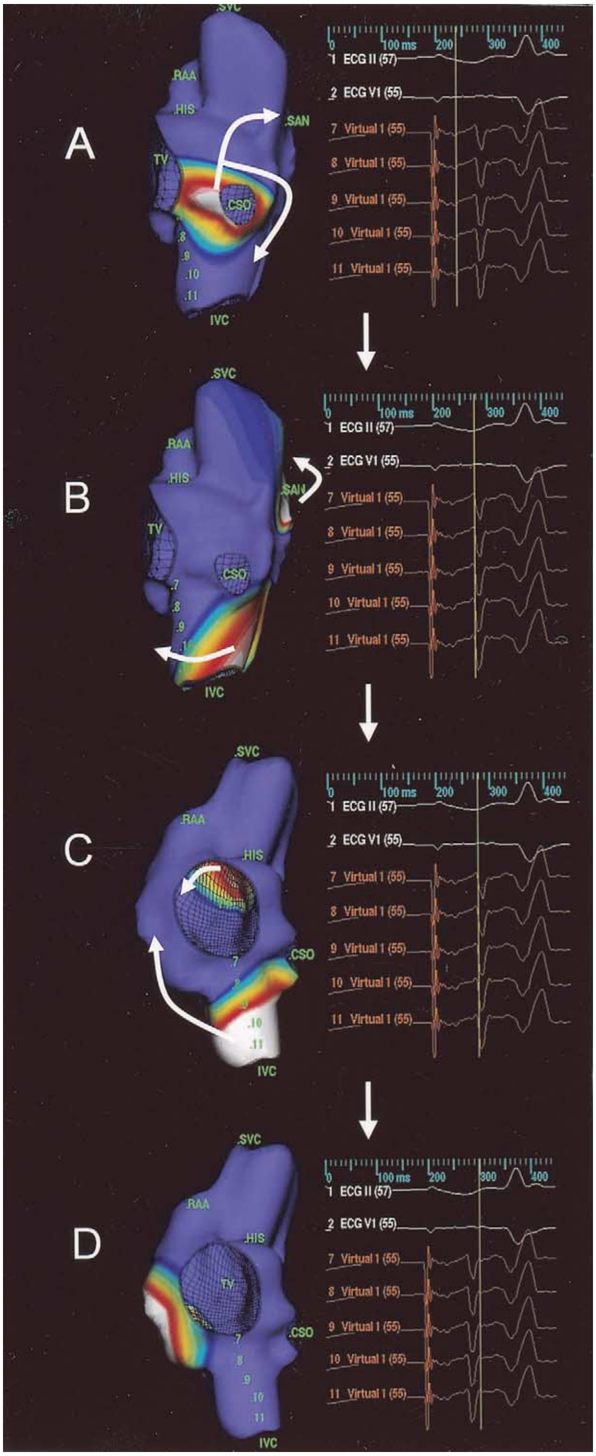

Figure 2. Incomplete cavotricuspid isthmus (CTI) block during coronary sinus pacing after ablation. **(A)** The activation wavefront originated in the coronary sinus ostium region with splitting of two wavefronts. **(B)** One activation wavefront propagated upward in the anterior septal wall to the roof, and the other wavefront proceeded downward in the posteroseptal wall to the CTI. **(C)** The upper wavefront crossed over the crista terminalis, and the lower wavefront traveled through the CTI. **(D)** Both wavefronts collided in the low anterolateral wall. The second component of virtual electrograms (virtual 7 to 11) showed an rS pattern.

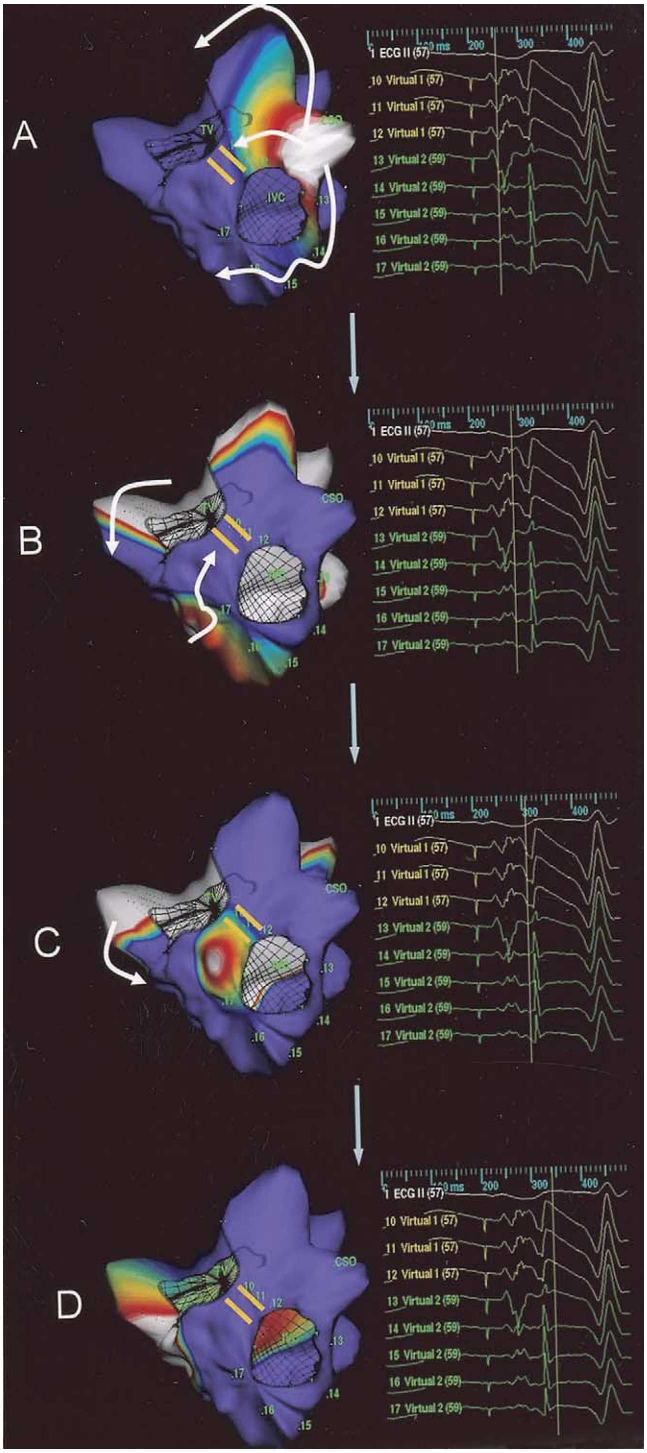

Figure 3. Complete cavotricuspid isthmus (CTI) block and transcristal conduction during coronary sinus pacing after ablation. **(A)** The activation wavefront originated in the coronary sinus ostium (CSO) region and split into two wavefronts. **(B)** One wavefront propagated upward in the septal wall to the roof, and the other wavefront crossed the gap of the crista terminalis. **(C)** The upper wavefront crossed over the top of crista terminalis, and the lower wavefront activated the CTI opposite the pacing site. **(D)** The upper wavefront propagated downward in the anterolateral wall. The second component of virtual electrograms (virtual 10 to 12) showed an rSR pattern.

Criteria of complete CTI conduction block. Because creation of complete CTI block can prevent recurrence of typical AFL, several mapping techniques have been proposed to demonstrate this criterion after RFA of the CTI (7–12). Initially, the activation mapping technique was used to show complete craniocaudal activation pattern of the opposite wall to the pacing site (7,8). Subsequently, complete CTI block was considered when a complete corridor of parallel double potentials from the right ventricle to the IVC was achieved (11). However, the presence of a very slow, persistent conduction through the ablation line can be misdiagnosed by both techniques; thus, differential pacing techniques must be used to allow determination of true CTI conduction block (16).

Recently, unipolar electrograms were demonstrated to be useful for determining the CTI block (12). Spach et al. (17,18) have shown that conduction along the longitudinal axis of the myocardial fibers produces RS or rS unipolar electrograms, and uniphasic unipolar R electrograms develop during termination of the activation wavefront. In this study, pacing from the CS before RFA resulted in RS or rS unipolar electrograms in the CTI. After RFA with complete CTI block (group I), the paced wavefront propagated around the TA to the other side of the ablation line. Therefore, the second component of double potentials at the ablation line showed an R or Rs pattern representing the wavefront termination at the ablation line. In contrast, during incomplete CTI block (group II), the wavefront can pass though the residual gap in the CTI; thus, the second component of double potentials can show an rS pattern representing an approaching and leaving activation wavefront.

CTI block with transcristal conduction. The CT has been demonstrated to be a posterior barrier in typical AFL (2–4). However, the presence of transcristal conduction during CS pacing was found by Arenal et al. (9) and Schumacher et al. (19). Using a basket catheter in the IVC orifice, Scaglione et al. (20) also found that 3 of 12 patients had a mimicking conduction through the CTI during CS pacing, which was due to conduction along the posterior part of IVC orifice. In this study, three patients showed complete CTI block with transcristal conduction during CS pacing. The second component of unipolar double potentials at the ablation line showed a characteristic rSR pattern. This unique finding has not been reported before. The rS deflection reflected the close-by activation wavefront due to transcristal conduction, and R wave represented the activation front propagating around the tricuspid annulus.

Conclusions. The study demonstrated the characteristics of virtual unipolar electrograms at the ablation line for detecting complete CTI block after RFA of typical AFL. A predominant R-wave pattern of the second component of unipolar double potentials at the ablation indicates complete CTI block, even in the presence of transcristal conduction.

Reprint requests and correspondence: Dr. Ching-Tai Tai, Division of Cardiology, Taipei Veterans General Hospital, 201 Sec. 2, Shih-Pai Road, Taipei, Taiwan. E-mail: ct.tai@msa.hinet.net.

REFERENCE

1. Puech P, Latour H, Grolleau R. Le flutter et ses limites. Arch Mal Coeur 1970;63:116–44.
2. Cosio FG, Lopez-Gil M, Arribas F, Palacios J, Goicolea A, Nunez A. Mechanisms of entrainment of human common atrial flutter studied with multiple endocardial recordings. Circulation 1994;89:2117–25.
3. Olgin JE, Kalman JM, Fitzpatrick AP, Lesh MD. Role of right atrial endocardial structures as barriers to conduction during human type I atrial flutter: activation and entrainment mapping guided by intracardial echocardiography. Circulation 1995;92:1839–48.
4. Shah DC, Jais P, Haissaguerre M, et al. Three-dimensional mapping of the common atrial flutter circuit in the right atrium. Circulation 1997;96:3904–12.
5. Feld GK, Fleck P, Chen PS, et al. Radiofrequency catheter ablation for treatment of human type I atrial flutter: identification of a critical zone in the reentrant circuit by endocardial mapping techniques. Circulation 1992;86:1233–40.
6. Lesh MD, Van Hare GF, Epstein LM, et al. Radiofrequency catheter ablation of atrial arrhythmias: results and mechanisms. Circulation 1994;89:1074–89.
7. Poty H, Saoudi N, Nair M, Anselme F, Letac B. Radiofrequency catheter ablation of atrial flutter: further insights into the various types of isthmus block: applications to ablation during sinus rhythm. Circulation 1996;94: 3204–13.
8. Tai CT, Chen SA, Chiang CE, et al. Long-term outcome of radiofrequency catheter ablation for typical atrial flutter: risk prediction of recurrent arrhythmias. J Cardiovasc Electrophysiol 1998;9:115–21.
9. Arenal A, Almendral J, Alday JM, et al. Rate-dependent conduction block of the crista terminalis in patients with typical atrial flutter: influence on evaluation of cavotricuspid isthmus conduction block. Circulation 1999;99:2771–8.
10. Anselme F, Savoure A, Cribier A, Saoudi N. Catheter ablation of typical atrial flutter: a randomized comparison of 2 methods for determining complete bidirectional isthmus block. Circulation 2001;103:1434–9.
11. Shah DC, Takahashi A, Jais P, Hocini M, Clementy J, Haissaguerre M. Local electrogram-based criteria of cavotricuspid isthmus block. J Cardiovasc Electrophysiol 1999;10:662–9.
12. Villacastin J, Almendral J, Arenal A, et al. Usefulness of unipolar electrograms to detect isthmus block after radiofrequency ablation of typical atrial flutter. Circulation 2000;102:3080–5.
13. Schmitt H, Weber S, Tillmanns H, Waldecker B. Diagnosis and ablation of atrial flutter using a high resolution, noncontact mapping system. Pacing Clin Electrophysiol 2000;23:2057–64.
14. Schneider MA, Ndrepepa G, Zrenner B, et al. Noncontact mapping-guided ablation of atrial flutter and enhanced-density mapping of the inferior vena cava-tricuspid annulus isthmus. Pacing Clin Electrophysiol 2001;24:1755–64.
15. Tai CT, Huang JL, Lin YK, et al. Noncontact three-dimensional mapping and ablation of upper loop re-entry originating in the right atrium. J Am Coll Cardiol 2002;40:746–53.
16. Shah D, Haissahuerre M, Takahashi A, Jais P, Hocini M, Clementy J. Differential pacing for distinguishing block from persistent conduction through an ablation line. Circulation 2000;102:1517–22.
17. Spach MS, Miller WT III, Geselowitz DB, Barr RC, Kootsey JM, Johnson EA. The discontinuous nature of propagation in normal canine cardiac muscle: evidence for recurrent discontinuities of intracellular resistance that affect the membrane currents. Circ Res 1981;48:39–54.
18. Spach MS, Miller WT III, Miller-Jones E, Warren RB, Barr RC. Extracellular potentials related to intracellular action potentials during impulse conduction in anisotropic canine cardiac muscle. Circ Res 1979;45:188–204.
19. Schumacher B, Jung W, Schmidt H, et al. Transverse conduction capabilities of the crista terminalis in patients with atrial flutter and atrial fibrillation. J Am Coll Cardiol 1999;34:363–73.
20. Scaglione M, Riccardi R, Calo L, et al. Typical atrial flutter ablation: conduction across the posterior region of the inferior vena cava orifice may mimic unidirectional isthmus block. J Cardiovasc Electrophysiol 2000;11:387–95.